

Prediction and Control of Blood Flow in the Human Brain Vascular Network

L. Yang, M. Xenos, L. Zhang, and A. A. Linninger

*Laboratory for Product and Process Design, Department of Bioengineering,
University of Illinois at Chicago, Chicago, IL 60607*

Often overlooked, millions of people are affected by cerebrovascular diseases such as Alzheimer's disease. Patients often do not receive a diagnosis early enough to get the full benefits of the treatments available today due to the similarities of symptoms between various cerebrovascular diseases. To address this problem, we propose a creation of a mathematical model of the cerebral vasculature. This paper primarily addresses the factors effecting blood flow distribution and the development of a control system that can eventually be applied to this model. An accurate mathematical model of the brain vasculature may allow an accurate simulation of different pathological conditions and phenomena of the brain, thus in the long term contributing to the study and treatment of cerebrovascular diseases.

Introduction

Applications

The brain vasculature system is defined as a vast system of blood vessels such as arteries, arterioles and veins in the brain. Each blood vessel is unique in its properties regarding its cross-sectional area, length, elasticity and its resistance and can be altered by the brain to control blood flow. This control of blood flow is crucial to the brain because it is the only way the brain can gather its energy since it does not have energy stores of its own. Figure 1 illustrates an image from a sagittal cut of the brain that is uploaded onto the software currently under development. The yellow highlights trace the arterial system of the brain and a network of tubes are drawn onto this highlight to recreate an accurate two-dimensional network of the arterial system. In order to further the development of this model we want to create a dynamic version which will allow us to model some of the phenomenon and pathologies affect the brain today. We will describe some general applications that we want to be able to model in the long term.

Cerebral Autoregulation

There are a few phenomena that take place in the brain that are only beginning to become uncovered. One of these phenomena is the cerebral autoregulation mechanism. The goal of cerebral autoregulation is to maintain the cerebral perfusion in spite of changes in the arterial pressure. Although the function of the cerebral autoregulation system is known, its mechanism remains elusive. New studies have shown that neurons, glial cells and vascular cells act together and constitute a single functional unit termed the neurovascular unit.²

We can see from Figure 2 that the astrocytes (glial cells) are located very close to the vascular cells (smooth muscle cells) and the neurons. The neurons can sense

changes in activity and relay a signal to the astrocyte which in turn will possibly release a variety of vasoactive mediators to the vascular cells near the walls of the blood vessel. The vascular cells then take up the neurotransmitter and converts the signal into an action in which the vascular cell will either dilate or constrict the designated blood vessel.²

Although the cerebral autoregulation mechanism can control blood flow through these vasomotor effectors, it can only control them to a certain extent. The ability of this autoregulation system to maintain a relatively constant cerebral blood flow is only when the cerebral perfusion pressure (CPP) is within the range of 50-170 *mmHg*.³ If the CPP is too high or too low, cerebral autoregulation ceases to function. The cerebral autoregulation mechanism is complicated further by its dependency on both the cerebral blood volume and the intracranial

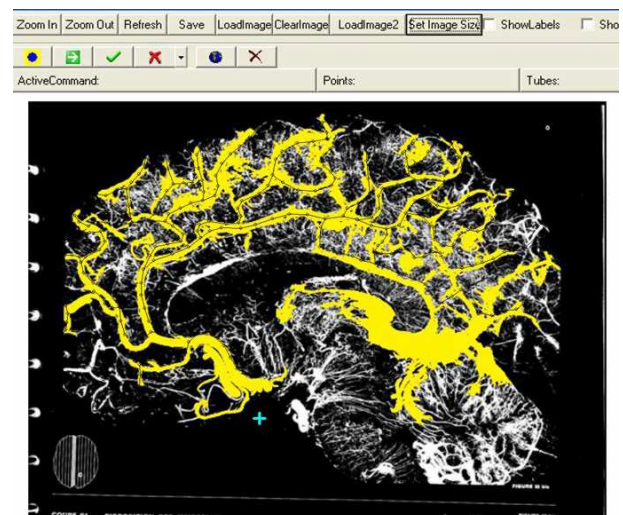


FIG. 1: Image of Sagittal Cut in the Brain. The yellow highlight describes the arterial system in the brain and the lines superimposed on the image represent the network of tubes drawn on by the network generator.¹

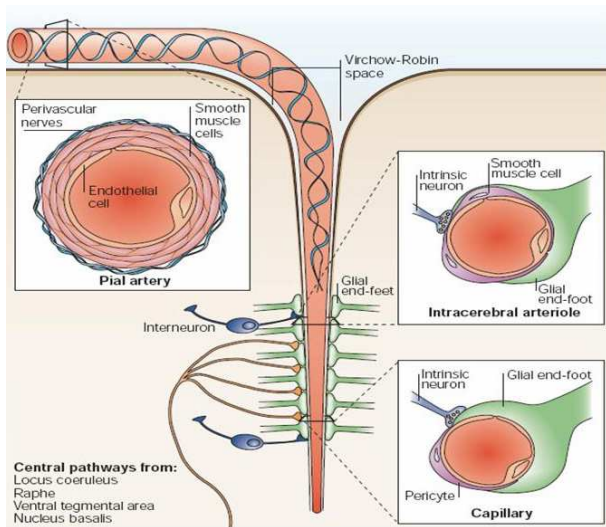


FIG. 2: Neurovascular Unit. Glial cells, vascular cells and neurons are oriented in respect to each other and thus why it is likely that they function together as a unit.²

pressure. A change in vessel diameter may also affect the intracranial pressure (ICP) through the changes in cerebral blood volume (CBV) and thus the ICP and CBV must be accounted for in an accurate model.⁴ The brain's ability to regulate the activity of neurovascular units allows it to perform other phenomena as well. Besides cerebral autoregulation, another phenomenon is the ability of the brain to divert blood flow to activated areas of the brain - functional hyperaemia.

Functional Hyperaemia

Functional hyperaemia is the ability of the brain to be able to divert flow to activated areas of the brain; this has been observed when an individual is moving, speaking, listening or in general thinking. As individuals are doing each of these actions, they are stimulating a specific part of their brain that is associated with those actions such as their auditory cortex (listening) and motor cortex (moving).⁵ It has been shown through fMRI data that certain parts of the brain will 'light' up as its being stimulated and will experience approximately an increase of approximately 400% in blood flow. Figure 3 shows an image taking through fMRI. This image shows the visual cortex being stimulated and the orange color represents the increase in blood flow to that area.

One of the proposed mechanisms for functional hyperaemia is termed intramural vascular signaling as shown in Figure 4. Due to the neurons sensing an increase in local activity, vascular cells such as smooth muscle cells in arterioles and pericytes in capillaries will dilate the local vasculature to allow greater blood flow. However, a local dilation of the smaller blood vessels will not in-

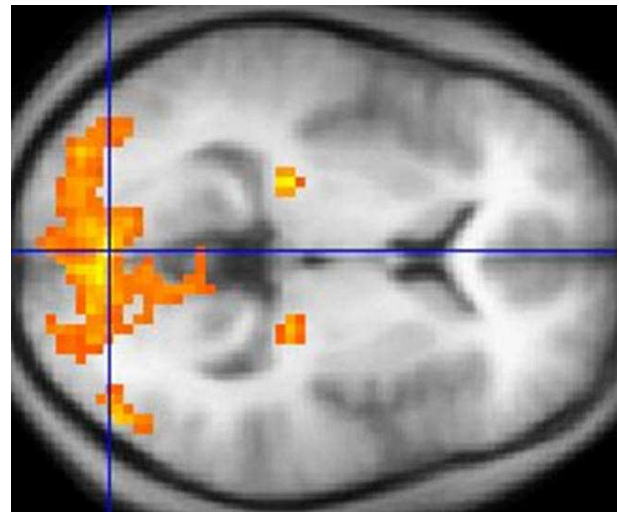


FIG. 3: fMRI image of the visual cortex. This illustration shows the increased blood flow towards a specific area of the brain, notably the visual cortex in this picture.

duce a sufficient amount of blood flow to the activated area. Thus, this local dilation will then in turn trigger a larger blood vessel further upstream such as a pial artery to dilate as well. The relaxation of both the local blood vessel and the larger blood vessel further upstream will induce a greater amount of blood flow that is sufficient for the activated area. Intramural vascular signaling proposes that the vasodilation of the lower blood vessel triggers a higher flow velocity in the upper branches. This higher flow velocity increases the shear stress of the upper branches, which in turn triggers a vasodilation response by the larger arteries to compensate for the increase in shear forces acting on the vascular walls.²

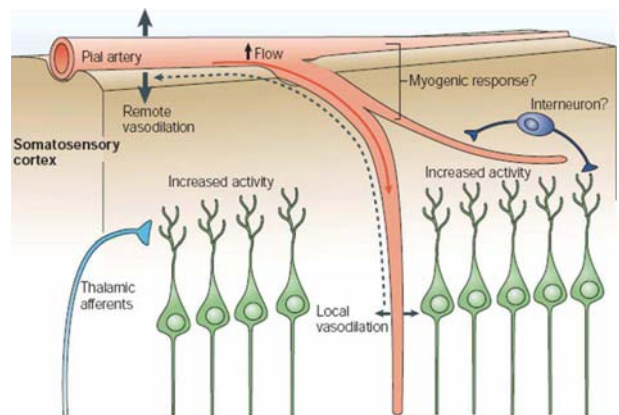


FIG. 4: Intramural vascular signaling. The local dilation propagates an increase in shear stress to the pial arteries upstream and triggers a vasodilation response by the pial arteries.²

toregulation and functional hyperaemia, we may be able to contribute to a better treatment for individuals who have lost these functions due to cerebrovascular disease.

Methods

Mathematical Description

Before we begin measuring the physical parameters of the blood vessels in the brain, we must first define the laws that govern our flow. The equations we use to govern fluid flow come from the principles of fluid dynamics.

$$\frac{\partial A}{\partial t} + \frac{\partial(AU)}{\partial x} = 0 \quad (1)$$

$$\frac{\partial U}{\partial t} + \frac{\partial}{\partial x} \left(\frac{U^2}{2} + \frac{P}{\rho} \right) = -F \quad (2)$$

$$P = E_L \left(\frac{A}{A_0} \right) \quad (3)$$

The frictional force (-F term) was then related to cross-sectional area and viscosity with the following relationship:

$$F = \frac{8\pi\mu Q}{A^2} \quad (4)$$

These equations were then incorporated into MATLAB (a computational program) to compute the physical parameters of a given network generated by the software that we're currently developing. As a side note, extensive research on cerebral haemodynamics has been done by electrical engineers as well. Although we will not discuss electrical analogies of cerebral haemodynamics in this paper, it may be useful to be able to correlate with research done by electrical engineers as to further the validation of this model. Linear equations are not just easier to solve, but they help bridge the physical model to the analogous electrical model.

Equation 1 is the mathematical representation of the conservation of mass termed the continuity equation. When a system is in steady state, the flow into the tube must be equal to the flow out of the tube. Thus, the continuity equation in our model guarantees that the entire system is in steady state. The second equation, Equation 2, is a mathematical representation of a conservation of momentum. We use the Navier-Stokes equation to relate different forces such as the frictional forces to velocities and pressures within our model. The last equation that will help determine how our flow is governed is the tube distensibility equation or Equation 3. This equation takes into account the fact that we're assuming that blood vessels can be represented as distensible tubes. Thus, we need to account for their elasticities and the effect of the shear forces the flow will exert on the walls of the tubes.

Transition to a Dynamic Model

The next step is to design a dynamic model for our network. The benefit of the dynamic model is so we can view the changes in blood flow distribution from changes in the physical parameters such as area and elasticity in real time and thus we can observe the intermediate changes in pressure and blood flow through out the given network. Before we can incorporate our dynamic changes into a complex network shown in the introduction, we have to use a simpler network but useful in testing the dynamic model to see if it works.

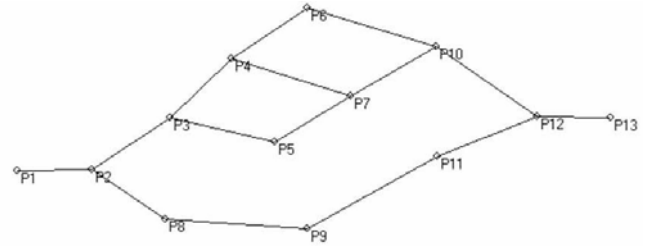


FIG. 6: Simple asymmetric network model generated by the Network Generator.

To make the transition from a static to a dynamic system we must introduce a time constant. The time constant regulates how long the dynamic simulation will go for and how often calculations are being done. Obviously, the smaller the time step the more accurate the model but the more time it will take for the computer to calculate the results. In order to test our dynamic model, we will demonstrate a series of tests in this paper. A tube will be constricted and the flow distribution will be analyzed at different points in the network to illustrate to us whether or not the model works. The dynamic model is based on the network illustrated in Figure 6. This network is meant to roughly represent the image the brain by being asymmetric in terms of the distribution of the tubes. The values for this network are uniform and can be seen in Table 1 to allow easier observation of the dynamic changes that occur in the flow distribution in our model. For the boundary conditions in this network we can either fix inlet flow and inlet pressure or inlet pressure and outlet pressure.

We constrict or decrease the diameter of the tube represented by P4 to P6 from three millimeters to two millimeters and view the dynamic changes in flow rate and pressures in tubes P8-P9, P10-P12 and P4-P6. This way we can observe changes that occur in the lower branch, upper branch and where the constriction is occurring.

Results

The blood vessel begins constricts linearly; beginning after 30 seconds have passed. Three different trials were

	Cross-Sectional Area (m^2)	Length (m)	Elasticity (Pa)
P1-P2	.003	1	1000
P2-P3	.003	1	1000
P2-P8	.003	1	1000
P3-P4	.003	1	1000
P3-P5	.003	1	1000
P4-P7	.003	1	1000
P4-P6	.003	1	1000
P5-P7	.003	1	1000
P6-P10	.003	1	1000
P7-P10	.003	1	1000
P8-P9	.003	1	1000
P9-P11	.003	1	1000
P10-P12	.003	1	1000
P11-P12	.003	1	1000
P12-P13	.003	1	1000

TABLE I: Parameters used within the model for each tube.

done on the network, each trial constricting the same tube but visualizing a different area in the network.

Simulation of the Lower Branch

From Figure 7, we can observe that after constricting P4-P6 from 3 mm to 2 mm we see that the mean flow rate have increased from $0.160 \frac{m^3}{s}$ to $0.162 \frac{m^3}{s}$ and the pressure increased from $120.34 Pa$ to $121.81 Pa$.

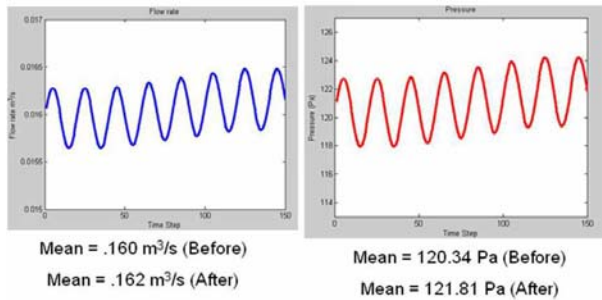


FIG. 7: Illustrates the flow rate and pressure in tube P8-P9 after constricting tube P4-P6.

Simulation of the Upper Branch

In this simulation shown in Figure 8, illustrates that in an upper branch we see a decrease in low rate from $0.0184 \frac{m^3}{s}$ to $0.0178 \frac{m^3}{s}$ and a decrease in pressure from $139 Pa$ to $134.56 Pa$.

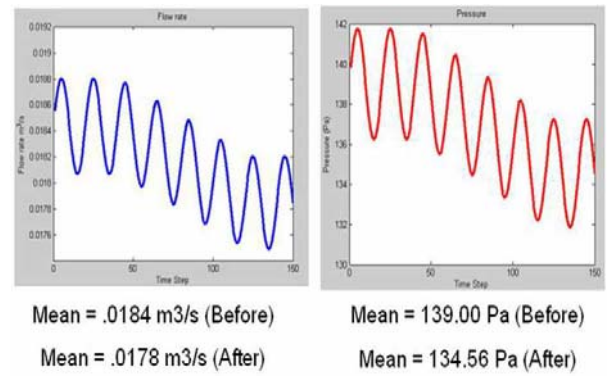


FIG. 8: Illustrates the flow rate and pressure in tube P10-P12 after constricting tube P4-P6.

Simulation of the Constricted Tube

We're also interested in the flow rate and pressure changes in the constricted tube as well. In Figure 9 we see that flow rate has decreased from $0.0076 \frac{m^3}{s}$ to $0.0055 \frac{m^3}{s}$ and pressure increased from $57.06 Pa$ to $93.36 Pa$.

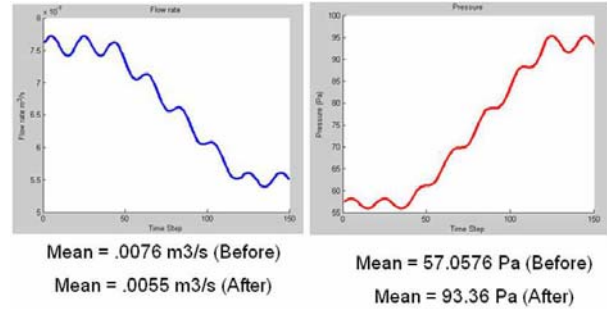


FIG. 9: Illustrates the flow rate and pressure in tube P4-P6 after constricting tube P4-P6.

Discussion and Conclusion

This simulation's purpose was to observe and analyze the results of flow rate and pressure to see if they would be supportive of the predictions. For the most part, the prediction is straightforward. All the bottom blood vessels are expected to show a net increase in pressure and flow rate. This is because after the constriction of P4 to P6 in the top half of the network, the net diameter of the entire top half has decreased compared to the bottom half. The flow must then get redistributed, in which a greater portion of the flow will distribute itself throughout the bottom region of the network. The net pressure and flow rate of the top half should decrease because there will be less flow designated to the upper half of the network.

The only special case of the behavior of blood flow is where the constriction actually takes place. The constriction reduces overall blood flow to the top half of the network thus reducing the blood flow to the constricted areas. However, because this area is mechanically being constricted, the pressure of that vessel will increase. Thus, unlike the other cases, we predict that the flow rate and pressure will change in opposite directions - with the flow rate decreasing and the pressure increasing.

The simulation data does support the prediction accurately so now the test can be taken a step further. The next step would be create a control system to be able to control either flow rate or pressure for various areas in a network thus allowing the potential modeling of different phenomena that can occur in the brain.

Based on the results of our simulations, it is reasonable to conclude that the model is indeed consistent qualita-

tively with what it is designed to do. So far, only a qualitative approach has been taken. The future approach will be to design a control system and actually implement physiologically consistent parameters into an even more complex network to see if it is indeed possible to divert blood flow to certain areas using real physiological data. Then eventually we can incorporate our model into an even more complex circuit such as the one shown in Figure 1 and determine if the simulations generated by the model are consistent with real experimental values.

Acknowledgements

I would like to thank the NSF-REU site at University of Illinois - Chicago and the Department of Defense for the funding. I would like to thank everyone in the lab for helping me out with any questions/problems I had.

-
- ¹ G. Salamon, *Atlas of the Arteries of the Human Brain*. (SANDOZ Editions, Paris, France, 1971).
 - ² C. Iadecola, *Nature Reviews Neuroscience* **5**, 347 (2004).
 - ³ R. Aaslid, K. F. Lindegaard, W. Sorteberg, and H. Nornes, *Stroke* **20**, 45 (1989).
 - ⁴ M. Ursino and C. A. Lodi, *American Journal Of Physiology-Heart And Circulatory Physiology* **43**, H1715 (1998).
 - ⁵ About Funtional MRI (www.fmri.org).
 - ⁶ National Institute of Neurological Disorders and Stroke (www.ninds.nih.gov).
 - ⁷ National Stroke Association (www.stroke.org).
 - ⁸ E. R. Kandel, J. H. Schwartz, and T. M. Jessell, *Principles of Neural Science* (Elsevier Science Publishing Co., New York, 1991), 3rd ed.
 - ⁹ World Health Organization (www.who.int/en/).

Appendix

Code For Dynamic Model (Figure 6)

Main Program Network

```

\clear;
clc;

%Boundary Conditions
P_INIT = 2000;
%Initial Pressure and part of both boundary conditions

T14_P = 1000; %Final Pressure
%T0_fi = .03;

T4_A0 = .003; %Preconstricted vessel diameter
Tcut = .002; %Constricted vessel diameter

%Parameters for autoregulation multiplier
M = 1.00001;
r = .003;

%Time steps
dt = 0.05;
dt2 = .005; %For the pulse drop
total_time = 150;

x0=ones(1,59);

for l = 1 : total_time

    time(l) = dt * l; %x-axis

    P_INIT(l) = 2000 * (1 + 0.01*sin(2.0*pi*time(l)));
    %Pressure Input

    %Calculates the unconstricted beginning
    if l < 40

```

```

options=optimset('Display','iter','MaxFuneval',
1e4);
% Option to display output
x = fsolve(@TubeLawEquationv1_time,x0,options,
P_INIT, T14_P,1,time); % Call optimizer
q = reformatv2_time(x,P_INIT,T14_P,1);
end

%Calculates the transition stage and constricted end
if l >= 40
options=optimset('Display','iter','MaxFuneval',
1e4);
% Option to display output
x = fsolve(@TubeLawEquationv2_time,x0,options,
P_INIT, T14_P, T4_A0, 1, time); % Call optimizer
q = reformatv2_time(x,P_INIT,T14_P,1);
if T4_A0 >= Tcut
T4_A0 = T4_A0 - T4_A0*dt2;
end

end
x(59) = T14_P;
x1(1) = q(13,1)
x2(1) = q(9,4) - q(13,4);

end

%Plots Data
figure(1)
plot(x1,'b', 'LineWidth', 3)
title('Flow rate')
xlabel('Time Step')
ylabel('Flow rate m^3/s')

figure(2)
plot(x2,'r','LineWidth', 3)
title('Pressure')
xlabel('Time Step')
ylabel('Pressure (Pa)')

Calculation of mean, max and min
A1 = max(x1) - min(x1)
max(x1)
min(x1)
mean = max(x1) - A1/2

A2 = max(x2) - min(x2)
max(x2)
min(x2)
mean = max(x2) - A2/2

Tube Law Function

function [Equ, z]=TubeLawEquation(x,
P_INIT,T14_P,1,time)
% Parameters *****

Pstar=1500;

u = .0027;
Young = 10000;

T0_l0=1.2401612798342;T1_l0=1.5587174214719;
T2_l0=1.41449637680695;T3_l0=1.78538511251774;
T4_l0=1.51433153569488;T5_l0=2.07480119529559;
T6_l0=1.47146185815331;T7_l0=2.23365171859894;
T8_l0=1.63975607942157; T9_l0=1.46996598600104;
T10_l0=2.3654175107156;T11_l0=2.47095123383688;
T12_l0=2.04156802482798;T13_l0=1.78639301386901;
T14_l0=1.22016392341357; T0_A0=.003;T1_A0=.003;
T2_A0=.003;T3_A0=.003;T4_A0=.003;T5_A0=.003;
T6_A0=.0025;T7_A0=.003;T8_A0=.003;T9_A0=.003;
T10_A0=.003;T11_A0=.003;T12_A0=.003;
T13_A0=.003;T14_A0=.003; T0_alfa=8*pi*u;
T1_alfa=8*pi*u;T2_alfa=8*pi*u;T3_alfa=8*pi*u;
T4_alfa=8*pi*u;T5_alfa=8*pi*u;T6_alfa=8*pi*u;
T7_alfa=8*pi*u;T8_alfa=8*pi*u;T9_alfa=8*pi*u;
T10_alfa=8*pi*u;T11_alfa=8*pi*u;
T12_alfa=8*pi*u;T13_alfa=8*pi*u;T14_alfa=8*pi*u;
T0_E=Young;T1_E=Young;T2_E=Young;T3_E=Young;
T4_E=Young;T5_E=Young; T6_E=Young;T7_E=Young;
T8_E=Young;T9_E=Young;T10_E=Young;T11_E=Young;
T12_E=Young;T13_E=Young;T14_E=Young;

% Variables *****
T1_fi=x(1);T2_fi=x(2);T3_fi=x(3);T4_fi=x(4);
T5_fi=x(5);T6_fi=x(6);T7_fi=x(7);T8_fi=x(8);
T9_fi=x(9);T10_fi=x(10);T11_fi=x(11);
T12_fi=x(12);T13_fi=x(13);T14_fi=x(14);
T0_fo=x(15);T1_fo=x(16);T2_fo=x(17);
T3_fo=x(18);T4_fo=x(19);T5_fo=x(20);
T6_fo=x(21);T7_fo=x(22);T8_fo=x(23);
T9_fo=x(24);T10_fo=x(25);T11_fo=x(26);
T12_fo=x(27);T13_fo=x(28);T14_fo=x(29);
T0_A=x(30);T1_A=x(31);T2_A=x(32);
T3_A=x(33);T4_A=x(34);T5_A=x(35);T6_A=x(36);
T7_A=x(37);T8_A=x(38);T9_A=x(39);T10_A=x(40);
T11_A=x(41);T12_A=x(42);T13_A=x(43);
T14_A=x(44);T0_P=x(45);T1_P=x(46);
T2_P=x(47);T3_P=x(48);T4_P=x(49);T5_P=x(50);
T6_P=x(51);T7_P=x(52);T8_P=x(53);
T9_P=x(54);T10_P=x(55);T11_P=x(56);
T12_P=x(57);T13_P=x(58);%T14_P=x(59);
T0_fi = x(59);

% Equations *****

%Continuity Eqns
Equ(1)=T0_fi -T0_fo;
Equ(2)=T1_fi -T1_fo;
Equ(3)=T2_fi -T2_fo;
Equ(4)=T3_fi -T3_fo;
Equ(5)=T4_fi -T4_fo;
Equ(6)=T5_fi -T5_fo;
Equ(7)=T6_fi -T6_fo;
Equ(8)=T7_fi -T7_fo;
Equ(9)=T8_fi -T8_fo;
Equ(10)=T9_fi -T9_fo;
Equ(11)=T10_fi -T10_fo;
Equ(12)=T11_fi -T11_fo;
Equ(13)=T12_fi -T12_fo;
Equ(14)=T13_fi -T13_fo;
Equ(15)=T14_fi -T14_fo;

%Tube Law Eqns
Equ(16)=(T0_P - Pstar) -T0_E * (T0_A/T0_A0 -1);
Equ(17)=(T1_P - Pstar) -T1_E * (T1_A/T1_A0 -1);
Equ(18)=(T2_P - Pstar) -T2_E * (T2_A/T2_A0 -1);

```

```

Equ(19)=(T3_P - Pstar) -T3_E * (T3_A/T3_A0 -1);
Equ(20)=(T4_P - Pstar) -T4_E * (T4_A/T4_A0 -1);
Equ(21)=(T5_P - Pstar) -T5_E * (T5_A/T5_A0 -1);
Equ(22)=(T6_P - Pstar) -T6_E * (T6_A/T6_A0 -1);
Equ(23)=(T7_P - Pstar) -T7_E * (T7_A/T7_A0 -1);
Equ(24)=(T8_P - Pstar) -T8_E * (T8_A/T8_A0 -1);
Equ(25)=(T9_P - Pstar) -T9_E * (T9_A/T9_A0 -1);
Equ(26)=(T10_P - Pstar) -T10_E * (T10_A/T10_A0 -1);
Equ(27)=(T11_P - Pstar) -T11_E * (T11_A/T11_A0 -1);
Equ(28)=(T12_P - Pstar) -T12_E * (T12_A/T12_A0 -1);
Equ(29)=(T13_P - Pstar) -T13_E * (T13_A/T13_A0 -1);
Equ(30)=(T14_P - Pstar) -T14_E * (T14_A/T14_A0 -1);

%N-S Eqns
Equ(31)=(P_INIT(1)-T0_P) -(T0_alfa/T0_A0^2)*T0_fi;
Equ(32)=(T0_P-T1_P) -(T1_alfa/T1_A0^2)*T1_fi;
Equ(33)=(T1_P-T2_P) -(T2_alfa/T2_A0^2)*T2_fi;
Equ(34)=(T1_P-T3_P) -(T3_alfa/T3_A0^2)*T3_fi;
Equ(35)=(T2_P-T4_P) -(T4_alfa/T4_A0^2)*T4_fi;
Equ(36)=(T2_P-T5_P) -(T5_alfa/T5_A0^2)*T5_fi;
Equ(37)=(T3_P-T6_P) -(T6_alfa/T6_A0^2)*T6_fi;
Equ(38)=(T4_P-T7_P) -(T7_alfa/T7_A0^2)*T7_fi;
Equ(39)=(T5_P-T8_P) -(T8_alfa/T8_A0^2)*T8_fi;
Equ(40)=(T0_P-T9_P) -(T9_alfa/T9_A0^2)*T9_fi;
Equ(41)=(T9_P-T10_P) -(T10_alfa/T10_A0^2)*T10_fi;
Equ(42)=(T10_P-T11_P) -(T11_alfa/T11_A0^2)*T11_fi;
Equ(43)=(T7_P-T12_P) -(T12_alfa/T12_A0^2)*T12_fi;
Equ(44)=(T11_P-T13_P) -(T13_alfa/T13_A0^2)*T13_fi;
Equ(45)=(T12_P-T14_P) -(T14_alfa/T14_A0^2)*T14_fi;

%Bifurcations and Unions
Equ(46)=(T0_fo +0) -(T1_fi +T9_fi +0);
Equ(47)=(T1_fo +0) -(T2_fi +T3_fi +0);
Equ(48)=(T2_fo +0) -(T4_fi +T5_fi +0);
Equ(49)=(T3_fo +0) -(T6_fi +0);
Equ(50)=(T4_fo +0) -(T7_fi +0);
Equ(51)=(T5_fo +T6_fo +0) -(T8_fi +0);
Equ(52)=(T5_P -T6_P);
Equ(53)=(T9_fo +0) -(T10_fi +0);
Equ(54)=(T10_fo +0) -(T11_fi +0);
Equ(55)=(T7_fo +T8_fo +0) -(T12_fi +0);
Equ(56)=(T7_P -T8_P);
Equ(57)=(T11_fo +0) -(T13_fi +0);
Equ(58)=(T12_fo +T13_fo +0) -(T14_fi +0);
Equ(59)=(T12_P -T13_P);

Reformat (for odd # of tubes) - Rearranges the
original array output into a matrix allowing
the output to be manipulated easier

function q = reformatv2_time(x, P_INIT, P,1)

t = (length(x) + 1)/4; %number of tubes
t1 = 1:t-1; %flow in's
t2 = t1(end)+1:t+t-1; %flow out's
t3 = t2(end)+1:t+t+t-1; %new areas
t4 = t3(end)+1:length(x);%Pressures
q = ones(t,4);

%Initializing flow ins
j = 1;
q(1,1) = x(t + 1);
for i = 2:t1(end) + 1
    q(i,1) = x(j);
    j = j + 1;
end

%Initializing flow outs
j = t2(1);
for i = 1:t
    q(i,2) = x(j);
    j = j + 1;
end

%Initializing areas
j = t3(1);
for i = 1:t
    q(i,3) = x(j);
    j = j + 1;
end

%Initializing pressure outs
j = t4(1);
q(t,4) = P;
z(1) = P_INIT(1);
for i = 2:t+1
    z(i) = x(j);
    j = j + 1;
end

j = 2;
for i = 1:t
    q(i,4) = z(j);
    j = j + 1;
end

j = 1;
for i = 1:t
    q(i,5) = z(j) - z(j+1);
    j = j + 1;
end
q(t,4) = P;

```